Running title: J. Costa et al., Polyamines during morphogenesis in hop

Arginine Decarboxilase expression, polyamines biosynthesis and reactive oxygen species during organogenic nodule formation in hop.

J. Costa[1a§], A. M. Fortes*[1a], J. M. Seguí-Simarro[2], A. Cordeiro[3], A. Tiburcio[3], T. Altabella[3], M. S. Pais[1]

[1] Unit of Molecular Biology and Plant Biotechnology- ICAT, FCUL, Campo Grande, 1749-016 Lisboa, Portugal; [2]Instituto de Conservación y Mejora de la Agrodiversidad Valenciana (COMAV), Universidad Politécnica de Valencia, Camino de Vera s/n, ed. 9B, 46022 Valencia, Spain; [3] Unitat de Fisiologia Vegetal, Facultat de Farmàcia, Universitat de Barcelona, Diagonal 643, 08028-Barcelona, Spain.

[a] These authors contributed equally to this paper.

* Corresponding author: Ana Margarida Fortes; Tel.: +351217500163; E-mail: amfortes@fc.ul.pt

§ Present location: Centre for Plant Sciences, Institute of Integrative and Comparative Biology, University of Leeds, United Kingdom.

Summary

Polyamines are involved in development and response to stress in plants. The biosynthesis of a common polyamine, putrescine, is controlled by arginine decarboxylase (ADC; EC 4·1.1·19). Wounding induces organogenic nodule formation from hop internodes (Fortes and Pais 2000). Here we show that ADC levels increase in response to internodes wounding and keep increasing until organogenic nodule formation after 28 days in culture. This was accompanied by a peak in putrescine levels especially in its free form (1323 nmol/ mg protein). During plantlet regeneration from nodules, the ratio between conjugated and free polyamines increases 2,95 fold comparing to that obtained for 15 days of culture. This increase in conjugated polyamines suggests that they are involved in plantlet regeneration or in the control of free polyamine levels.

Reactive oxygen species increase in tissues surrounding nodules and nodular areas where separation into daughter-nodules is occurring. The high levels of putrescine may serve as a source of H_2O_2 which may in turn act as a signaling molecule for plantlet regeneration.

Immunogold labeling revealed that ADC is located in plastids, nucleus and cytoplasm of nodular cells. In vacuolated cells ADC immunolabelling in plastids doubles that of proplastids of meristematic cells. Location of ADC in different subcellular compartments may indicate its role in metabolic pathways taking place in these compartments.

Altogether these data suggest that polyamines play a role in organogenic nodule formation. Reactive oxygen species may either constitute a physiological response to the stress inherent to *in vitro* culture conditions, or be the trigger of this morphogenic process in hop.

Keywords: arginine decarboxilase; *Humulus lupulus*; organogenic nodule; polyamines; reactive oxygen species

Abbreviations: ADC arginine decarboxilase; DAB Diaminobenzidine; DAO diamine oxidase; NBT nitroblue tetrazolium; ODC ornitine decarboxilase; PAO polyamine oxidase; PAs polyamines; Put putrescine; ROS reactive oxygen species; SAMDC *S*-adenosyl-L-methionine decarboxylase; Spd spermidine; Spm spermine.

Introduction

Polyamines are ubiquitous small aliphatic amines that occur in living organisms either as free cations or conjugates with phenolic acids and polyanionic macromolecules (Galston, 1990). The most common polyamines are spermidine and spermine, together with their diamine precursor putrescine. Polyamines are related to important developmental phenomena, including cell growth and division (Chattopadhyay, 2002; Theiss, 2002), morphogenesis (Fos, 2003; Paschalidis, 2001; Pedroso, 1997), stabilization of nucleic acids and membranes (Thomas, 2001), protein synthesis and chromatin function (Mattheus, 1993) and biotic and abiotic stresses (see review (Bouchereau, 1999). Polyamines also serve as precursors of several classes of alkaloids (Flores, 1982; Hashimoto, 1994) which may play important roles in plant defense against herbivores.

The biosynthesis of polyamines is controlled primarily by three enzymes: ornithine decarboxylase (ODC; EC 4·1.1·17) and arginine decarboxylase (ADC; EC 4·1.1·19), which are responsible for the production of putrescine, and *S*-adenosyl-L-methionine decarboxylase (SAMDC; EC 4·1.1·50), which is necessary for the synthesis of spermidine and spermine. It has been postulated that ornithine decarboxylase is active during cell proliferation whereas arginine decarboxylase is stimulated in response to stress (Smith, 1990). Polyamines are catabolized mostly by diamine and polyamine oxidases (Smith, 1985). Diamine oxidase (DAO, EC 1·4.3·6), which is found mainly in Leguminosae, catabolizes putrescine to form pirroline, hydrogen peroxide and ammonia, whereas polyamine oxidase (PAO, EC 1·.5.3.·3), which is found in the monocotyledonous plants, oxidizes spermidine or spermine forming pyrroline, diamine propane and hydrogen peroxide or diazabicyclononane, diamine propane and hydrogen peroxide, respectively (Federico and Angelini 1991). It is likely that plants have acquired the ability to produce putrescine (put) via ADC to meet specific requirements during normal development and also during adaptation to environment (Bouchereau et al. 1999) such as in response to stress and in wound or hormone response. The involvement of polyamines in stress response has been reported for several plant species, although their precise role is still unclear. Spermidine (spd) and spermine (spm) present anti-senescent properties (Besford et

al. 1993) and yet, they may inhibit growth and induce oxidative stress (Zacchini and Agazio 2001). Recently, it was shown that spd and spm increased nitric oxide release in *Arabidopsis thaliana* seedlings (Tun et al. 2006). It was demonstrated that manipulation of the polyamine biosynthetic pathway, through expression of *Datura adc* gene in transgenic rice confers tolerance to drought stress (Capell et al. 2004). Exposure of plant cells to stress is associated with oxidative damage at cellular level. The reactive oxygen species (ROS), including H_2O_2, are responsible for the oxidative stress. As hydrogen peroxide is a product of polyamine catabolism, earlier authors correlated phenomena such as programmed cell death in animal cells (Ha et al. 1997) or cell wall differentiation in maize mesocotyl (Laurenzi et al. 1999) with an increase of PAO activity. On the other hand, ROS, particularly H_2O_2, can act as a signaling molecule that regulates plant development, stress adaptation, and programmed cell death (Apel and Hirt 2004). It is known that PAs are capable of protecting membranes against ROS-induced lipid peroxidation (Tadolini 1988). Polyamines inhibit NADPH oxidase-mediated superoxides generation (Papadakis and Roubelakis- Angelakis 2005).

Oxidative stress may affect the regenerating potential of plant protoplasts and inevitably the protoplast fate (re-entry into cell cycle or cell death) (Papadakis and Roubelakis- Angelakis 2002). However, oxidative stress may also play a role in plant morphogenesis. In the case of *Vitis vinifera*, H_2O_2 reduces regeneration potential, but contrastingly H_2O_2 is required for protoplast division (de Marco and Roubelakis 1996).

Somatic embryogenesis and organogenic nodule formation are important morphogenic processes. Nodular structures have been studied in several plant species and were found to be an additional morphogenic pathway useful for regeneration strategies, automated micropropagation, and genetic transformation for desirable characteristics (McCown et al. 1988). The lack of efficient protocols for some agricultural plants and trees is a major limitation for their improvement through genetic engineering. Therefore, it is important to continue research towards understanding factors involved on *in vitro* plant regeneration. Organogenic nodule formation and the involvement of wounding in their induction have been previously described in hop (*Humulus lupulus* L.) (Fortes and Pais 2000; Fortes et al. 2004; Silva et al. 2004).

In this study, we present data suggesting a link between wound-induced organogenic nodule formation and ADC expression, polyamines biosynthesis and reactive oxygen species formation.

Materials and Methods

Plant material and culture conditions

The internodes from *Humulus lupulus* (var. Nugget) plants, maintained under *in vitro* conditions, were morphologically induced according to the protocol previously described (Fortes and Pais 2000). Internodes of 6-9 mm long were wounded throughout by several incisions (3-5) using a razor blade (wounding treatment) before inoculation in MS medium (Murashige and Skoog, 1965). Material was sampled at the following morphogenic stages: internodes at the time of excision from the parent plant; 12, 24 and 48 hours upon internodes inoculation; 4 and 7 days after culture initiation corresponding to divisions in cambial and cortical cells of internodal explants; 15 days on culture medium in which several prenodular structures are formed inside the *calluses*; 28 days after culture initiation corresponding to nodule formation; 45 days on culture medium in which plantlet regeneration occurs from organogenic nodules.

Histochemical detection of ROS

Plant material from the different assay conditions and culture time-points was incubated under vacuum in sodium phosphate buffer 10 mM (pH 7.8) containing NBT 0.5% (w/v), NADPH 10 μM and EDTA 10 μM (Doke and Ohashi, 1988). After remaining 15 minutes under light and at room temperature the samples were transferred to chloric hydrate solution (2.5 g/ml) and maintained at 4ºC until observation under magnifying lenses (CETI, Belgium) and photographed [Minolta (X-300 S) and Kodak film (100 ASA)].

Hydrogen peroxide was detected in plant material by incubation in DAB-HCl solution (1 mg/ml) (pH 3.8) (Sigma, MO, USA; # D-8001) for 5–10 minutes in the dark, after which the material was transferred to ethanol 96% (v/v) and maintained at 4ºC until observation. Control internodes with 15 days in culture were incubated in DAB-HCl solution supplemented with catalase 1000 U/ml and treated as described above.

Extraction of proteins and immunoblot analysis

Proteins were extracted as previously described (Fortes et al. 2004) using an extraction buffer as described by Borrel et al. (1996). Proteins were subjected to electrophoresis on a discontinuous gradient of SDS-polyacrylamide consisting of a 12 % (w/v) acrylamide resolving gel and a 6 % (w/v) stacking gel. Thirty μg total protein was loaded per lane together with prestained standard proteins.

After electrophoresis, proteins were transferred to Immobilon membranes (Millipore; Bedford, MA) and an equal loading was confirmed by Ponceau S staining. For the immunodetection, membranes were incubated for 2 h at room temperature with a rabbit polyclonal antibody raised against tobacco (Bortolloti et al. 2004) diluted 1:2000 in the blocking buffer (2% powdered skimmed milk, 0.05% Tween-20 in PBS). After rinses in washing buffer, membranes were incubated for 2 h with alkaline phosphatase-conjugated anti-rabbit IgG (Boehringer Mannheim), diluted 1:1000 in the blocking buffer. Finally, the proteins recognized by the antibody were revealed by treatment with a NBT-BCIP mixture. Controls were made, by replacing the first antibody with pre-immune serum.

Immunocytochemistry and quantification of immunogold labeling

Samples were fixed overnight at 4ºC in 4% (w/v) paraformaldehyde in phosphate buffered saline (PBS). After three PBS washes (5 min each), samples were dehydrated in a methanol series at 4ºC, washed in pure methanol, infiltrated and embedded in Lowicryl K4M at -30ºC and finally polymerized under UV irradiation. Semithin (2 μm-thick) sections were obtained for preliminary histological analysis. For immunogold labeling, Lowicryl ultrathin (~100 nm) sections were collected on formvar- and carbon-coated nickel grids.

Immunogold labeling was performed essentially as previously described (Seguí-Simarro et al. 2004). Grids carrying Lowicryl ultrathin sections were sequentially floated on drops of double-distilled water and PBS for few minutes, and 5% BSA (bovine serum albumin) in PBS for 5 minutes. Then, grids were incubated for 1 hr at room temperature with the same anti-ADC antibody used for the immunoblot analyses, diluted 1:10 in 1% BSA in PBS. After three washes in PBS containing 1% BSA, sections were incubated with a goat anti-rabbit IgG conjugated to 10-nm colloidal gold (BioCell; Cardiff, UK) diluted 1:25 in 1% BSA in PBS for 45 min. Finally, grids were washed, air-dried, counterstained with 5% aqueous uranyl acetate and lead citrate, and observed in a Philips CM10 transmission electron microscope operating at 100 kV. Two different controls were performed in parallel, either by excluding the anti-ADC antibody or substituting it by preimmune serum. Quantification of immunogold labeling was designed as previously described (Seguí-Simarro et al. 2004). Sampling was carried out over a number of micrographs randomly taken from different cells (corresponding to 28 days of culture) on each grid. The number of micrographs was determined using the progressive mean test (Seguí-Simarro and Staehelin 2006), with a minimum confidence limit of 0.05. Labeling density was defined as the number of particles per area unit (μm^2). This number of particles was determined by hand counting particles over the compartments under study (cytoplasm, nucleus, and plastids). Estimation of background was performed over cell walls, vacuoles, starch deposits and resin. The area in μm^2 was measured using a square lattice composed of 11 x 16 squares of 15 x 15 mm each. For each cell type and subcellular compartment, labeling density was expressed as mean labeling density of all micrographs_± S.D., and statistically compared using a *Student's t*-test, with $\alpha \leq 0.05$.

Quantification of polyamines

Plant material was extracted in 5% (w/v) TCA (600 mg plant material/ ml TCA). The homogenates were centrifuged for 20 min at 13 000 rpm. The bound amines in the supernatant, and the insoluble amines in the pellet (resuspended in the original volume of NaOH 1 M) were released by treating the fractions with 6 N HCl at 110 °C for 18 h in a sealed ampule. After heating, the samples were centrifuged for 5 min at 13 000 rpm, dried

under a stream of air at 80 °C, and resuspended in TCA. TCA extracts were analysed for free, soluble and insoluble PAs following dansylation. The dansylation mixture consisted of 200 μl TCA extract (equivalent to about 20 mg fresh tissue), 400 μl dansyl chloride (5 mg ml^{-1} in acetone; Sigma, St. Louis, Missouri, USA), and 200 μl saturated Na_2CO_3. After overnight incubation at room temperature the reaction was stopped by addition of 100 μl proline (100 mg ml^{-1}). Dansylpolyamines were extracted in 0.5 ml of toluene by collecting the organic phase, drying and dissolving in 0.8 ml of acetonitrile. Finally the samples were filtered through a 0.45 µm filter. The standard sample was treated as described above and consisted of a mixture of 0.05 mM diaminopropane, putrescine, cadaverine, 1,7-diaminoheptane, spermidine and spermine. Aliquots were analyzed by reversed-phase HPLC (Marcé et al. 1995) using the system HPLC (PHENOMEX, U.S.A). The dansylpolyamines injected in the column [Sphereclone 5 µm ODS (2), 250 x 4,60 m^2, ser#386140] were eluted in a gradient of acetonitrile and water of 70% (v/v) acetonitrile and 30% water for 5 min, 100% (v/v) acetonitrile for 4 min, 70% (v/v) acetonitrile and 30% water for 5,5 min, after which the initial conditions were re-established in the chromatography system (Applied Biosystems, USA). Elution of the dansylpolyamines was performed at 25^0C with a flow rate of 1.5 $ml.min^{-1}$ and monitored at 252 nm.

Results

Wounding of internodes leads to ADC protein accumulation which increases throughout organogenic nodule formation

Western blot analysis was carried out to evaluate ADC expression and accumulation during induction and formation of organogenic nodules. At the time of internodes inoculation two bands with a molecular mass of approximately 24 kD and 54 kD corresponding to ADC protein were detected. The 54 kD protein kept approximately constant throughout the different morphogenic stages, except for the stage of prenodule when a considerable increase in its levels was noticed. During the first week, when divisions are occurring in cambial and cortical cells of internodes (Fortes and Pais 2000), ADC protein level constantly increased mainly due to an increase in the 24 kD protein. In

nodules which appear 28 days upon internode inoculation, this ADC isoenzyme reached its highest level, then dropping to non detectable levels at about 45 days after inoculation of internodes (Fig.1), during plantlet regeneration from nodules. The 54 kD protein also decreased at this morphogenic stage, though to a lower extent than the 24 kD protein (Fig. 1).

Subcellular localization of ADC in plastids, cytoplasm and nucleus

The subcellular localization of the ADC protein in different cell types was analyzed by immunogold labelling in three time points during organogenic nodule formation: 7 days of culture (Fig. 2), 28 days of culture corresponding to nodules formation (Figs. 3, 4) and 45 days of culture corresponding to plantlet regeneration (data not shown). Seven days upon wounding cell divisions are occurring in cambial and cortical cells (Fig. 2 A, B). Cortical cells were surrounded by degenerating cells, probably undergoing cell death (Fig. 2B arrow). Gold particles appeared over the nucleus, cytoplasm and plastids of cortical cells but not in vacuoles and Golgi stacks (Fig. 2C). Immunogold labeling also appeared in the nucleus and cytoplasm of both meristematic (Figs. 3A-C) and differentiated nodular cells (Figs. 4A-C). Gold particles appeared dispersed throughout the cytoplasm as well as in plastids (Figs. 3C, 4A, 4B). In the nucleus, signal was found dispersed at the interchromatin region and sometimes at the borders of condensed chromatin masses (Fig. 4A). As long as the ultrastructure of plastid membranes can be discerned in Lowicryl-embedded samples, gold particles were never found on grana, labeling being restricted to the stroma (Fig. 4B). Signal was rarely or not found over other cytoplasmic organelles as vacuoles or cell wall (Figs. 4A, B). Controls excluding the anti-ADC antibody or substituting it by preimmune serum did not show significant labelling over any subcellular region (Fig. 4C).

In order to obtain detailed information regarding the different subcellular distribution of ADC in proliferative versus highly vacuolated nodular cells (Figs. 3, 4), immunogold labeling was quantified in both cell types. Unspecific background signal was also quantified over the cell walls, vacuoles, starch deposits and resin present in the micrographs, and it never exceeded 5% of the estimated signal. For both proliferating and differentiated cells (Fig. 5), immunogold particles were twice more abundant in cytoplasm

than in nucleus, being the mean labeling density not statistically different ($\alpha \leq 0.05$) between both cell types (0.7±0.30 particles/cytoplasmic μm^2 and 0.3±0.24 particles/nuclear μm^2 in proliferating cells, and 0.8±0.38 particles/cytoplasmic μm^2 and 0.4±0.21 particles/nuclear μm^2 in vacuolated cells). However, the mean labeling density was significantly different in the case of plastids, where almost twice the mean labeling density was found in plastids of vacuolated cells versus those of proliferating cells (1.2±0.65 and 0.7±0.28 particles/μm^2, respectively), suggesting that in differentiated cells, ADC accumulates in plastids.

Increase in polyamines during nodule formation

During organogenic nodule induction, all three PAs were present both in free and conjugated forms (Fig. 6 A-C). The most abundant PA throughout the process was Put either in free or conjugated forms. The exception was for the TCA-insoluble fraction (Fig. 6C) in which Spd was found in an higher concentration at days 28 and 45 (1,6 and 1,9 fold higher, respectively). Spm presented the lowest concentration in all three fractions quantified (free, TCA-soluble and TCA-insoluble conjugated). In all three forms Put content started to increase from day 4, peaking at day 28 and declining at day 45. Spd and Spm showed a similar profile though the increase in these PAs was more moderate up to day 15. The time-course analysis of the contents of all three PAs (Put, Spd and Spm) showed a similar trend in the different fractions being the TCA-insoluble conjugates detected only in small amounts comparing to both free and soluble conjugated PAs (Fig. 6C). Changes in the ratio between free and conjugated forms during organogenic nodule formation are shown in Fig. 7. At day 15 the level of free PAs was 1.55 fold higher comparing to the conjugated forms. From day 28 onwards there was a marked enhancement in the level of conjugated PAs, with a shift on the ratio between conjugated and free forms from 0,7 at day 15 to 1,62 at day 28 and 1,92 at day 45. This shift was mainly due to soluble and insoluble conjugated forms of Spd (Fig. 6 B, C). Interestingly, though the amounts of soluble conjugates of Spd are much higher than insoluble conjugates of Spd after 28 days (960,99 nmol mg protein^{-1} and 118,02 nmol mg protein^{-1} respectively), the insoluble conjugates showed an higher increase in between days 15 and 28 (27,0 fold comparing to 18,2 fold). During the period of 15 and 28 days total free PAs increased 5,2

fold whereas total soluble and insoluble conjugates increased 9,3 and 10,7 fold respectively.

In situ staining of reactive oxygen species

Immediately after excision of internodes from the parental plant, ROS production could be observed scattered throughout the internode (Fig. 8A). Twenty-four hours after internodes inoculation, increase in ROS was detected mainly in areas previously submitted to wounding as shown by NBT treatment (Fig. 8B arrow). The *in situ* detection of hydrogen peroxide, as early as 12h after culture initiation, showed a strong DAB staining restricted to the wounded areas (not shown). After 7 days in solid medium, the explants started forming *calli* in the previously wounded regions (Fortes and Pais, 2000). These structures appeared dark purple after NBT treatment (Fig. 8C arrow). After 15 days in culture, NBT staining was observed mainly in *calli* cells and in prenodular structures (Fig. 8D, E). DAB staining also showed that hydrogen peroxide accumulation intensified from the inner to the outer layers of prenodules (Fig. 8F). During nodule development ROS production could be observed in regions of future nodule separation (Fig. 8G black arrow) and in *calli* tissues formed due to proliferation of explant cells and that surround nodular clusters (Fig. 8G white arrow). Nodule separation appears to be initiated by the formation of a necrotic layer at the region of future nodule separation which accumulates reactive oxygen species (Fortes 2003).

Discussion

Polyamines are involved in developmental processes, including cell growth and division (Chattopadhyay et al. 2002; Theiss et al. 2002) and morphogenesis (Paschalidis et al. 2001; Fos et al., 2003). In hop internode cultures, we describe a high increase in total PAs content four days after culture initiation, probably related to the onset of active cambial and cortical cell division. Polyamine synthesis, abundance, and distribution seem to correlate positively with cell division (Paschalidis and Roubelakis-Angelakis 2005, Gemperlová et al. 2005). Sugar beet cell suspension cultures have shown marked increases in both Put and Spd after stimulation of quiescent cells to cell division (Fowler et al. 1996).

According to Papadakis et al. (2005), totipotent-tobacco protoplasts, with high division rates, have the highest level of endogenous PAs. Total Put predominates over Spd and Spm during organogenic nodule induction and formation in hop. This is in accordance with the results obtained by Papadakis et al. (2005) for totipotent-protoplasts. Recalcitrant-grapevine protoplasts showed a lower PA content and the higher ratio of Spm to total PAs which suggests that the levels and metabolism of the intracellular PAs could be related to the expression of totipotency of plant protoplasts (Papadakis et al. 2005). It may be that PAs play a role in the expression of determination for organogenic nodule formation in hop. In fact, PAs content kept increasing up to nodule formation reaching huge values at this time point. Polyamines have also been related to other morphogenic processes such as somatic embryogenesis (Pedroso et al. 1997, Bertoldi et al. 2004). In embryogenic regions of Camellia leaves, the time course PAs content suggested that soluble and insoluble conjugated Put and soluble conjugated Spd are related to the formation and development of globular embryos (Pedroso et al. 1997). Recently, PAs were suggested to be involved in polar auxin transport, in the differentiation of vascular tissues and in the definition of vein positions (Clay and Nelson 2005). It may be that the huge amount of PAs detected in hop nodules 28 days after culture initiation are also related to differential auxin fluxes inside nodules which may lead to organization of nodular vascular centers to which future regenerated plantlets will be connected to (Fortes and Pais 2000). Hop nodules contain higher levels of IAA than internodes (Filipa Santos, personal communication) which support the proposed role of PAs in differential auxin fluxes.

In protein extracts of hop internodes and nodules the anti-ADC antibody from tobacco detected two bands with approximate molecular masses of 54 and 24 kD. In protein extracts of tobacco leaves, the anti-ADC antibodies detected a band with approximate molecular mass of 77 kD, and a smaller band of 54 kD. The 54 kD protein may be an ADC form present only in the chloroplast of photosynthetic tissues (Bortolloti et al. 2004). The recognition in hop extracts of a band of a molecular mass of 24 kD using a tobacco polyclonal antibody is not surprising since it has also been reported for other plant species such as oat (Borrel et al. 1995), where ADC is synthesized as a pre-protein of 66 KD, which is cleaved to produce a fragment of 42 KD (containing the original amino terminus) and a 24 KD polypeptide (containing the original carboxyl terminus), these two processed

polypeptides being held together by disulfide bonds (Malmberg et al. 1992, Malmberg and Cellino 1994).

During organogenic nodule formation in hop, depending on the tissue, ADC is located in three different compartments: nucleus, plastids and cytosol. ADC activity has been localized mainly in the chloroplast of photosynthetic tissues and in the nucleus of the non-photosynthetic tissues (Bortolotti et al. 2004). The subcellular localization of ODC and ADC indicate that both proteins are also active in cytosolic fraction (Gemperlová et al. 2005). This differential subcellular localization observed in plant cells was also shown for ODC in animal tissues (Schipper et al. 1999) and may be cell type-specific and/or dependent on the physiological status (Schipper and Verhofstad 2004).

ADC can play different roles depending on its subcellular localization (Bortoloti et al. 2004). Its presence in chloroplast may be related to photosynthesis. Beigbeder et al. (1995) have demonstrated a correlation between PA concentration, chlorophyll biosynthesis and photosynthetic rate. In organogenic nodules differentiated cells containing chloroplasts present more ADC in that cellular compartment than proliferating cells in plastids, suggesting that in those cells PAs may be related to photosynthesis. Studies in mammalian cells showed direct binding of PAs to nucleic acids and ability to modulate their conformation and interaction with proteins, playing a role in cellular signaling (Thomas and Thomas 2001). It may be that ADC presence in nucleus as reported here may play such a role.

In hop, wounding of internodes for organogenic nodule induction led to accumulation 12 hours after induction of the 24 kD protein, whereas the 54 kD protein remained constant at this stage. This result suggests that 24 kD isoenzyme may be important in response to an abiotic stress such as wounding. The product of ADC, putrescine, also increased already 12 hours upon internodes inoculation. ADC activity has been linked to stress responses (Galston et al. 1997, Koetje et al. 1993). It is known that PAs are capable of protecting membranes against ROS-induced lipid peroxidation (Tadolini 1988). Recently, arginine decarboxylase and ornithine decarboxylase genes were expressed in apple cells and stressed shoots (Hao et al. 2005). According to these authors *ADC* expression correlates with cell growth and stress responses to chilling, salt, and dehydration, suggesting that ADC is a primary biosynthetic pathway for putrescine biosynthesis in apple.

Levels of ADC protein, both 54 kD and 24 kD isoenzymes, kept increasing during the morphogenic stages of prenodules and nodules suggesting the role of ADC and its product on morphogenesis. The fact that the 24 kD protein is not detected 45 days after culture initiation and the 54 kD protein decreased at this stage may suggest a feed-back regulation of *de novo* synthesis of ADC. Immunogold labeling also detected ADC after 45 days although at a low extent (not shown). Since Put levels also decreased drastically it may be that Put is oxidized and serve as a source of H_2O_2 or alternatively may form conjugates as suggested by an increased ratio of conjugated versus total PAs 45 days after culture initiation.

During plantlet regeneration from organogenic nodules (after 45 days) the ratio conjugated/ total PAs increases 2,95 and 1,18 fold comparing to 15 and 28 days of culture respectively. This increase in conjugated forms is mainly due to the increase in conjugated Spd. Conjugated amines accumulate dramatically in response to certain developmental or stress factors (Scoccinati et al. 2000). Polyamines conjugation seems to be advantageous for the long-term regulation of free PA levels because the risk of accumulation of harmful metabolites, produced by oxidative deamination, is reduced (Cvikrova et al. 1999, 2003). Jasmonates have been shown to induce over-accumulation of methylputrescine and conjugated PAs in *Hyoscyamus muticus* L. root cultures (Biondi 2000). Fortes et al. (2005) showed that jasmonic acid and its precursor 12-oxophytodienoic acid increased in hop nodules after 45 days of culture. This increase in jasmonic acid may thus influence the relative accumulation of conjugated PAs or may stimulate their oxidation through activation of diamine oxidase (Biondi 2003). Fortes et al. (2004) showed there is an increase in lipid peroxides (precursors of jasmonates) during plantlet regeneration from organogenic nodules which is related to an increase in reactive oxygen species content. According to Federico and Angelini (1991), an increase in DAO activity leads to generation of hydrogen peroxide. This compound may lead to subsequent triggering of programmed cell death (Apel and Hirt 2004). A programmed cell death may be taking place in tissues surrounding nodules, which may provide an extra source of carbon and nitrogen for the growing plantlets. In fact, H_2O_2 could be noticed in necrotic areas leading to nodule separation and mainly in surrounding calli tissues.

Reactive oxygen species are not only stress signal molecules, but are also an intrinsic signal in plant growth and development (Van Breusegem et al. 2001). Generation of superoxide anions can induce lipid peroxidation, leading to loss of membrane integrity and finally to tissue necrosis. Fortes (2003) showed that explants determined for organogenesis have more lipid peroxides than explants cultures in medium without growth regulators which never developed nodules. Preliminary experiments showed that internodes treated with 10 mM N- acetyl-cysteine, an efficient antioxidant, never formed organogenic nodules. Only *calli* structures and incipient prenodules were developed. However, when 0,4 mM N- acetyl-cysteine was used no effect in nodule formation was observed (data not shown). These results suggest that there is a minimal threshold of ROS concentration for morphogenic processes to occur.

The link between oxidative stress and morphogenesis has been previously described for somatic embryogenesis (Thybaud-Nissen et al. 2003). These authors suggest that the arrangement of new cells into organized structures might depend on a genetically controlled balance between cell proliferation and cell death. Oxidative status increases during formation of spruce embryos (Stasola and Yeung 1999, 2001). Obert et al. (2005) showed that morphogenesis can be regulated by compounds that change oxidative status such as desferrioxamine and hydroxynonenal. Under extreme conditions, somatic cells have to change their fate: either they have to die (apoptosis) or dedifferentiate and divide (Feher et al. 2002) and afterwards differentiate and form organs or somatic embryos. Thus, there is a strong indication that somatic embryogenesis is a stress response (Pretova and Obert 2003). Our data also suggest that organogenic nodule formation in hop is a stress responsive morphogenic process and both ROS and PAs are involved in this process.

Acknowledgements

The authors would like to thank Dr. Rubén Alcázar (Barcelona, Spain) for help with measurements of polyamines. This work was supported by the Portuguese Foundation for Science and Technology, by a PhD grant (PRAXIS XXI/BD/19536/99) and a Post-Doc grant to Ana M. Fortes (SFRH/BPD/13850/2003). Joana Costa was supported by the Project PCII/1999/BME/32734 (FCT). AFT acknowledges the support from the European

Union (EU-QLK5-CT-2002-00841) and from Spanish Ministerio de Educación y Ciencia (BIO2005-09252-C02-01).

References

Apel K, Hirt H (2004) Reactive Oxygen species: Metabolism, Oxidative Stress, and Signal Transduction. Ann. Rev. Plant Biol. 55**:**373-399

Beigbeder A, Vavadakis M, Navakoudis E, Kotzabasis K (1995) Influence of Polyamine Inhibitors on Light-Independent and Light-Dependent Chlorophyll Biosynthesis and on the Photosynthetic Rate. J. Photochem. Photobiol. B-Biology 28**:**235-242

Bertoldi D, Tassoni A, Martinelli L, Bagni N (2004) Polyamines and somatic embryogenesis in two *Vitis vinifera* cultivars. Physiol. Plant. 120**:**657-666

Besford RT, Richardson CM, Campos JL, Tiburcio AF (1993) Effect of polyamines on stabilization of molecular complexes in thylakoid membranes of osmotically stressed oat leaves. Planta 189**:**201-206

Biondi S, Fornale S, Oksman-Caldentey KM, Eeva M, Agostani S, Bagni N (2000) Jasmonates induce over-accumulation of methylputrescine and conjugated polyamines in *Hyoscyamus muticus* L. root cultures. Plant Cell Rep. 19**:**691-697

Biondi S, Scoccianti V, Scaramagli S, Ziosi V, Torrigiani P (2003) Auxin and cytokinin modify methyl jasmonate effects on polyamine metabolism and ethylene biosynthesis in tobacco leaf discs. Plant Science 165**:**95-101

Borrell A, Besford RT, Altabella T, Masgrau C, Tiburcio AF (1996) Regulation of arginine decarboxylase by spermine in osmotically stressed oat leave. Physiol. Plant. 98**:**105-110

Borrell A, Culianez-Macia FA, Altabella T, Besford RT, Flores D, Tiburcio AF (1995) Arginine Decarboxylase Is Localized in Chloroplasts. Plant Physiol. 109**:**771-776

Bortolotti C, Cordeiro A, Alcazar R, Borrell A, Culianez-Macia FA, Tiburcio AF, Altabella T (2004) Localization of arginine decarboxylase in tobacco plants. Physiol. Plant. 120**:**84-92

Bouchereau A, Aziz A, Larher F, Martin-Tanguy J (1999) Polyamines and environmental challenges: recent development. Plant Science 140**:**103-125

Capell T, Bassie L, Christou P (2004) Modulation of the polyamine biosynthetic pathway in transgenic rice confers tolerance to drought stress. PNAS 101**:**9909-9914

Chattopadhyay MK, Tabor CW, Tabor H (2002) Absolute requirement of spermidine for growth and cell cycle progression of fission yeast (*Schizosaccharomyces pombe*). PNAS 99**:**10330-10334

Clay NK, Nelson T (2005) Arabidopsis thick vein Mutation Affects Vein Thickness and Organ Vascularization, and Resides in a Provascular Cell-Specific Spermine Synthase Involved in Vein Definition and in Polar Auxin Transport. Plant Physiol. 138**:**767-777

Cvikrova M, Binarova P, Eder J, Vagner M, Hrubcova M, Zon J, Machackova I (1999) Effect of inhibition of phenylalanine ammonia-lyase activity on growth of alfalfa cell suspension culture: Alterations in mitotic index, ethylene production, and contents of phenolics, cytokinins and polyamines. Physiol. Plant. 107**:**329-337

Cvikrova M, Mala J, Hrubcova M, Eder J, Zon J, Machackova I (2003) Effect of inhibition of biosynthesis of phenylpropanoids on sessile oak somatic embryogenesis. Plant Physiol. Biochem. 41**:**251-259

de Marco A, Roubelakis-Angelakis KA (1996) The Complexity of Enzymic Control of Hydrogen Peroxide Concentration May Affect the Regeneration Potential of Plant Protoplasts. Plant Physiol. 110**:**137-145

Doke N, Ohashi Y (1988) Involvement of an O-2-Generating System in the Induction of Necrotic Lesions on Tobacco-Leaves Infected with Tobacco Mosaic-Virus. Physiol. Mol. Plant Pathol. 32**:**163-175

Federico R, Angelini R (1986) Occurrence of diamine oxidase in the apoplast of pea epicotyls. Planta 167**:**300-302

Federico R, Angelini R (1991) Polyamine catabolism in plants. In: Slocum RD, Flores HE (ed) Biochemistry and Physiology of Polyamines in Plants. CRC Press, Boca Raton, FL, pp 41–56

Feher A, Pasternak T, Otvos K, Miskolczi P, Dudits D. (2002) Induction of embryogenic competence in somatic plant cells a review. Biologia 57 5–12

Flores HE, Galston A (1982) Polyamines and Plant Stress: Activation of Putrescine Biosynthesis by Osmotic Shock. Science 217**:**1259-1261

Fortes AM (2003) Organogenic nodule formation in hop (Humulus lupulus var. Nugget). A contribution for the understanding of morphogenesis in plants. PhD thesis, Science Faculty, University of Lisbon, Portugal

Fortes AM, Coronado MJ, Testillano PS, Risueno MdC, Pais MS (2004) Expression of Lipoxygenase During Organogenic Nodule Formation from Hop Internodes. J. Histochem. Cytochem. 52**:**227-241

Fortes AM, Miersch O, Lange PR, Malho R, Testillano PS, Risueno MdC, Wasternack C, Pais MS (2005) Expression of Allene Oxide Cyclase and Accumulation of Jasmonates during Organogenic Nodule Formation from Hop (*Humulus lupulus* var. Nugget) Internodes. Plant Cell Physiol. 46**:**1713-1723

Fortes AM, Pais MS (2000) Organogenesis from internode-derived nodules of *Humulus lupulus* var. Nugget (*Cannabinaceae*): histological studies and changes in the starch content. Am. J. Bot. 87**:**971-979

Fos M, Proano K, Alabadi D, Nuez F, Carbonell J, Garcia-Martinez JL (2003) Polyamine Metabolism Is Altered in Unpollinated Parthenocarpic pat-2 Tomato Ovaries. Plant Physiol. 131**:**359-366

Fowler MR, Kirby MJ, Scott NW, Slater A, Elliott MC (1996) Polyamine metabolism and gene regulation during the transition of autonomous sugar beet cells in suspension culture from quiescence to division. Physiol. Plant. 98**:**439-446

Galston AW, Sawhney KR, Altabella T, Tiburcio AF (1997) Plant polyamines in reproductive activity and response to abiotic stress. Botanica Acta 110**:**197-207

Gemperlova L, Eder J, Cvikrova M (2005) Polyamine metabolism during the growth cycle of tobacco BY-2 cells. Plant Physiol. Biochem. 43**:**375-381

Ha HC, Woster PM, Yager JD, Casero RAJr. (1997) The role of polyamine catabolism in polyamine analogue-induced programmed cell death. PNAS 94**:**11557-11562

Hao Y-J, Kitashiba H, Honda C, Nada K, Moriguchi T (2005) Expression of arginine decarboxylase and ornithine decarboxylase genes in apple cells and stressed shoots. J. Exp. Bot. 56**:**1105-1115

Hashimoto T, Yamada Y (1994) Alkaloid Biogenesis: Molecular Aspects. Ann. Rev. Plant Physiol. Plant Mol. Biol. 45:257-285

Koetje DS, Kononowicz H, Hodges TK (1993) Polyamine metabolism associated with growth and embryogenic potential in rice. J. Plant Physiol. 141:215-221

Laurenzi M, Rea G, Federico R, Tavladoraki P, Angelini R (1999) De-etiolation causes a phytochrome-mediated increase of polyamine oxidase expression in outer tissues of the maize mesocotyl: a role in the photomodulation of growth and cell wall differentiation. Planta 208:146-154

Malmberg RL, Cellino ML (1994) Arginine decarboxylase of oats is activated by enzymatic cleavage into two polypeptides. J. Biol. Chem. 269:2703-2706

Malmberg RL, Smith KE, Bell E, Cellino ML (1992) Arginine Decarboxylase of Oats Is Clipped from a Precursor into Two Polypeptides Found in the Soluble Enzyme Plant Physiol. 100:146–152

Mattheus MR (1993) Polyamines, Chromatin Structure and Transcription. Bioessays 15:561-567

McCown BH (1988) Adventitious rooting of tissue cultured plants. In: Davis TD, Haissig BE, Sankhla N (ed) Adventitious root formation in cuttings. Diocorides, Portland, pp 289-302.

Murashige I, Skoog F (1962) A revised medium for rapid growth and bioassays with tobacco tissue cultures. Physiol. Plant. 15:473-497

Obert B, Benson EE, Millam S, Pretova A, Bremner DH (2005) Moderation of morphogenetic and oxidative stress responses in flax in vitro cultures by hydroxynonenal and desferrioxamine. J. Plant Physiol. 162:537-547

Papadakis AK, Paschalidis KA, Roubelakis-Angelakis KA (2005) Biosynthesis profile and endogenous titers of polyamines differ in totipotent and recalcitrant plant protoplasts. Physiol. Plant. 125:10-20

Papadakis AK, Roubelakis-Angelakis KA (2002) Oxidative stress could be responsible for the recalcitrance of plant protoplasts .Plant Physiol. Biochem. 40:549-559

Paschalidis KA, Roubelakis-Angelakis KA (2005) Sites and Regulation of Polyamine Catabolism in the Tobacco Plant. Correlations with Cell Division/Expansion, Cell Cycle Progression, and Vascular Development. Plant Physiol. 138:2174-2184

Paschalidis KA, Aziz A, Geny L, Primikirios NI, Roubelakis-Angelakis KA (2001) Polyamines in grapevine. In: Roubelakis-Angelakis KA (ed) Molecular biology and biotechnology of the grapevine. Kluwer Academic, Dordrecht, pp 109–151.

Pedroso MC, Primikirios N, Roubelakis-Angelakis KA, Pais MS (1997) Free and conjugated polyamines in embryogenic and non embryogenic leaf regions of camellia leaves before and during direct somatic embryogenesis. Physiol. Plant. 101**:**213-219

Pretova A, Obert B (2003) Flax (*Linum usitatissimum* L.) — A plant system for study of embryogenesis. Acta Biol Cracov Bot 45 15–18

Schipper RG, Cuijpers VMJI, de Groot LHJM, Thio M, Verhofstad AAJ (2004) Intracellular Localization of Ornithine Decarboxylase and Its Regulatory Protein, Antizyme-1.J. Histochem. Cytochem. 52**:**1259-1266

Schipper RG, Romain N, Otten AA, Tan J, Lange WP, Verhofstad AAJ (1999) Immunocytochemical Detection of Ornithine Decarboxylase. J. Histochem. Cytochem. 47**:**1395-1404

Scoccianti V, Sgarbi E, Fraternale D, Biondi S (2000) Organogenesis from *Solanum melongena* L. (eggplant) cotyledon explants is associated with hormone-modulated enhancement of polyamine biosynthesis and conjugation. Protoplasma 211**:**51-63

Segui-Simarro JM, Staehelin LA (2006) Cell cycle-dependent changes in Golgi stacks, vacuoles, clathrin-coated vesicles and multivesicular bodies in meristematic cells of *Arabidopsis thaliana*: A quantitative and spatial analysis. Planta 223**:**223-236

Segui-Simarro JM, Austin JR, White EA, Staehelin LA (2004) Electron Tomographic Analysis of Somatic Cell Plate Formation in Meristematic Cells of Arabidopsis Preserved by High-Pressure Freezing. Plant Cell 16**:**836-856

Silva MF, Fortes AM, Testillano P, Risueño MC, Pais MS (2004) Differential expression and cellular localization of ERKs during organogenic nodule formation from internodes of *Humulus lupulus* var. Nugget. Eur. J. Cel. Biol. 83 (8):425-433.

Smith TA (1985) Polyamines. Ann. Rev. Plant Physiol. 36**:**117-143

Smith TA (1990) Plant polyamines: metabolism and functions. In: Flores HE, Arteca RN, Shannon JC (ed) Polyamines and Ethylene: Biochemistry, Physiology, and Interactions. American Society of Plant Physiologists, Rockville, pp 1-17

Stasolla C, Yeung EC (1999) Ascorbic acid improves conversion of white spruce somatic embryos. In Vitro Cellular and Developmental Biology - Plant 35**:**316-319

Stasolla C, Yeung EC (2001) Ascorbic acid metabolism during white spruce somatic embryo maturation and germination. Physiol. Plant. 111**:**196-205

Tadolini B (1988) Polyamine inhibition of lipoperoxidation: the influence of polyamines on iron oxidation in the presence of compounds mimicking phospholipid polar heads. Biochem. J. 249**:**33-36

Theiss C, Bohley P, Voigt J (2002) Regulation by polyamines of ornithine decarboxylase activity and cell division in the unicellular green alga *Chlamydomonas reinhardtii*. Plant Physiol. 128**:**1470-1479

Thibaud-Nissen F, Shealy RT, Khanna A, Vodkin LO (2003) Clustering of Microarray Data Reveals Transcript Patterns Associated with Somatic Embryogenesis in Soybean. Plant Physiol. 132**:**118-136

Thomas T, Thomas J (2001) Polyamines in cell growth and cell death: molecular mechanisms and therapeutic applications. Cel. Mol. Life Scien. (CMLS) 58**:**244-258

Tun NN, Santa-Catarina C, Begum T, Silveira V, Handro W, Floh EIS, Scherer GFE (2006) Polyamines Induce Rapid Biosynthesis of Nitric Oxide (NO) in *Arabidopsis thaliana* Seedlings. Plant Cell Physiol. pci252

Van Breusegem F, Vranova E, Dat J, FInze D (2001) The role of active oxygen species in plant signal transduction. Plant Science 161**:**405-414

Zacchini M, Marotta A, de Agazio M (1997) Tolerance to salt stress in maize callus lines with different polyamine content. Plant Cell Rep. 17**:**119-122

Figures legends

Fig.1. Immunoblot analysis of ADC. Protein extracts corresponding to several morphogenic stages are represented (0, 12 and 24 hours, and 7, 15, 28 and 45 days upon wounding). 30 μg total protein extract was loaded per lane.

Fig. 2 a-c. Anti-ADC immunogold labeling in hop internodes after seven days of culture. **a** Semi-thin section showing divisions in cortical (Ct) and cambial cells (Cb). **b** Ultra-thin section showing cortical cells undergoing division and surrounded by cells undergoing cell death (arrow). **c** Ultra-thin section showing labeling in the cytoplasm (cyt), nucleus (n) and plastids (p). Labelling is absent in vacuoles (v) and golgi vesicles (g). Bars: **a** = 100 μm; **b** = 2,5 μm; **c** = 500 nm.

Fig. 3 a-c. Anti-ADC immunogold labeling in meristematic nodular cells after 28 days of culture. **a** Semi-thin section showing meristematic (McCown) and vacuolated cells (Vc) of nodules. **b** Magnification of meristematic cells. **c** Meristematic cell showing gold particles over nucleus, cytoplasm and plastids. Bars: **a** = 100 μm; **b** = 400 nm; **c** = 300 nm.

Fig. 4 a-c. Anti-ADC immunogold labeling in differentiated nodular cells after 28 days of culture. **a** and **b** Differentiated cells, highly vacuolated, showing significant labeling in the cytoplasm, nucleus and plastids. No labeling is observed in cell wall (cw) and vacuoles (v). **c** Control of immunogold labeling with preimmune anti-ADC. Bar in Fig. **a** = 250 nm. Bars in Figs. **b**, **c**= 1 μm

Fig. 5. Histogram representing labeling density in different cellular compartments of nodular cells following anti-ADC immunolocalization. In proliferating cells labeling density is similar in plastids and cytoplasm. Plastids showed the highest labeling density in vacuolated nodular cells.

Fig. 6. Changes in polyamines levels (Put, Spd and Spm) during organogenic nodule formation and plantlet regeneration in hop. (A) Free forms. (B) TCA-soluble conjugates.

(C) TCA-insoluble conjugates. Each value represents the mean of three independent experiments ± S.E.

Fig. 7. Total amount of free and conjugated polyamines during organogenic nodule formation and plantlet regeneration in hop. Each value represents the mean of three independent experiments ± S.E.

Fig. 8. Tissue specific distribution of ROS following staining with NBT (**a**-**e**, **g**) and DAB (**f**). **a** Internode at the time of excision from the parent plant. Dark purple spots identifying ROS are seen. **b** Internode 24 hours upon wounding showing intense NBT staining at the cutting regions. **c** Internode seven days upon wounding. *Calli* cells concentrated in previously wounded areas show intense NBT staining (arrow). **d** Aspect of a prenodule (pn) arising 15 days upon internodes inoculation showing cells stained dark purple. **e** Internode 15 days upon wounding showing prenodules with intense accumulation of ROS. **f** Internode section showing a prenodule stained with DAB. **g** Cluster of nodules (n) 45 days after internodes inoculation. Initial explant (e) has proliferated giving rise to *calli* cells which appeared intensively stained (white arrow). Bars in Figs. **a, b, c** and **f** = 0.6 cm. Bar in Fig. **e** = 0.3 cm. Bars in Figs. **f, g** = 0.5 cm.

Joana Costa
Fig.1

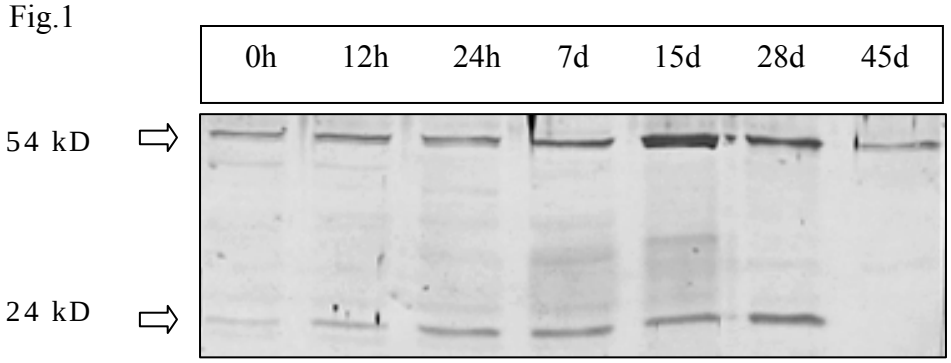

Joana Costa
Fig. 2

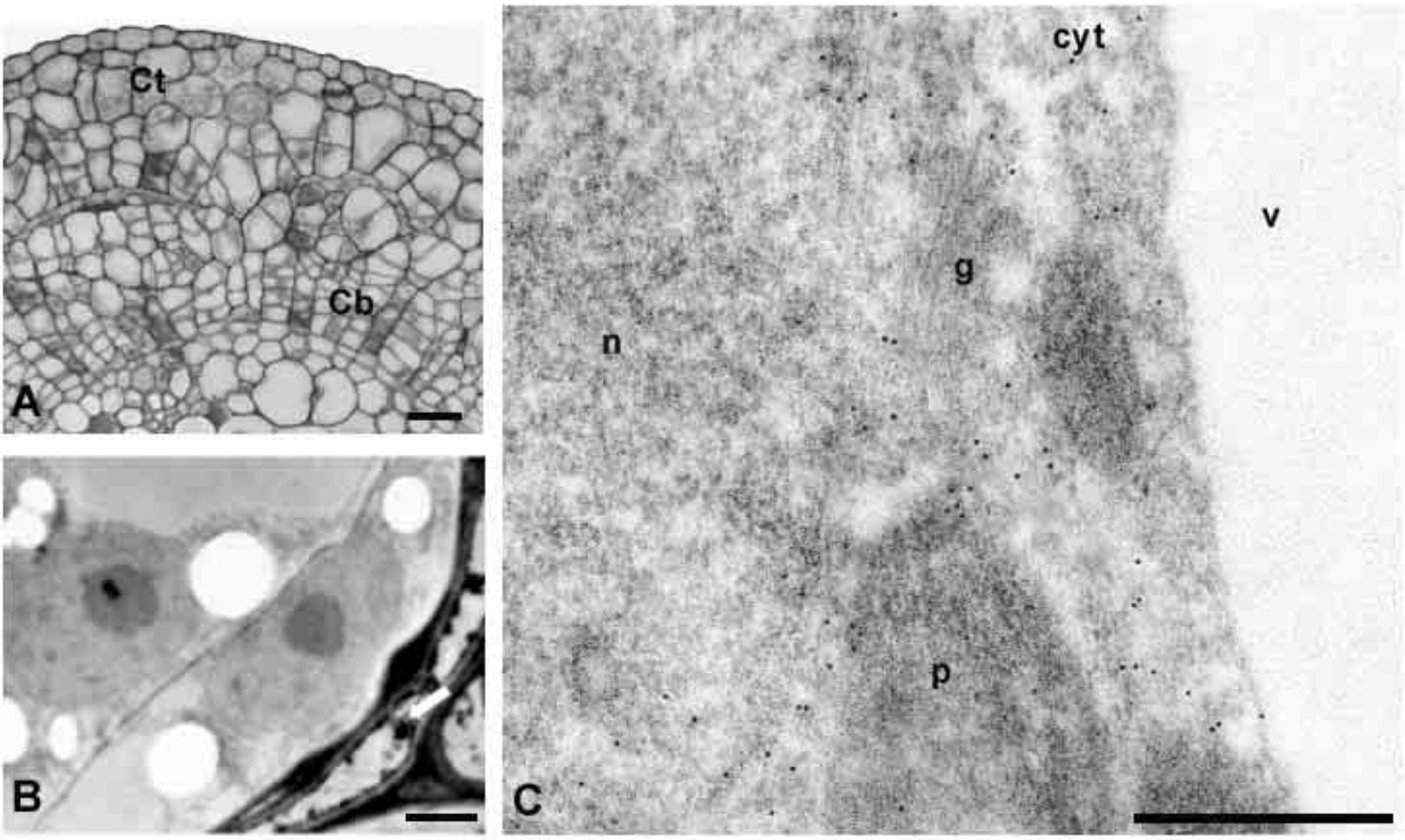

Joana Costa
Fig. 3

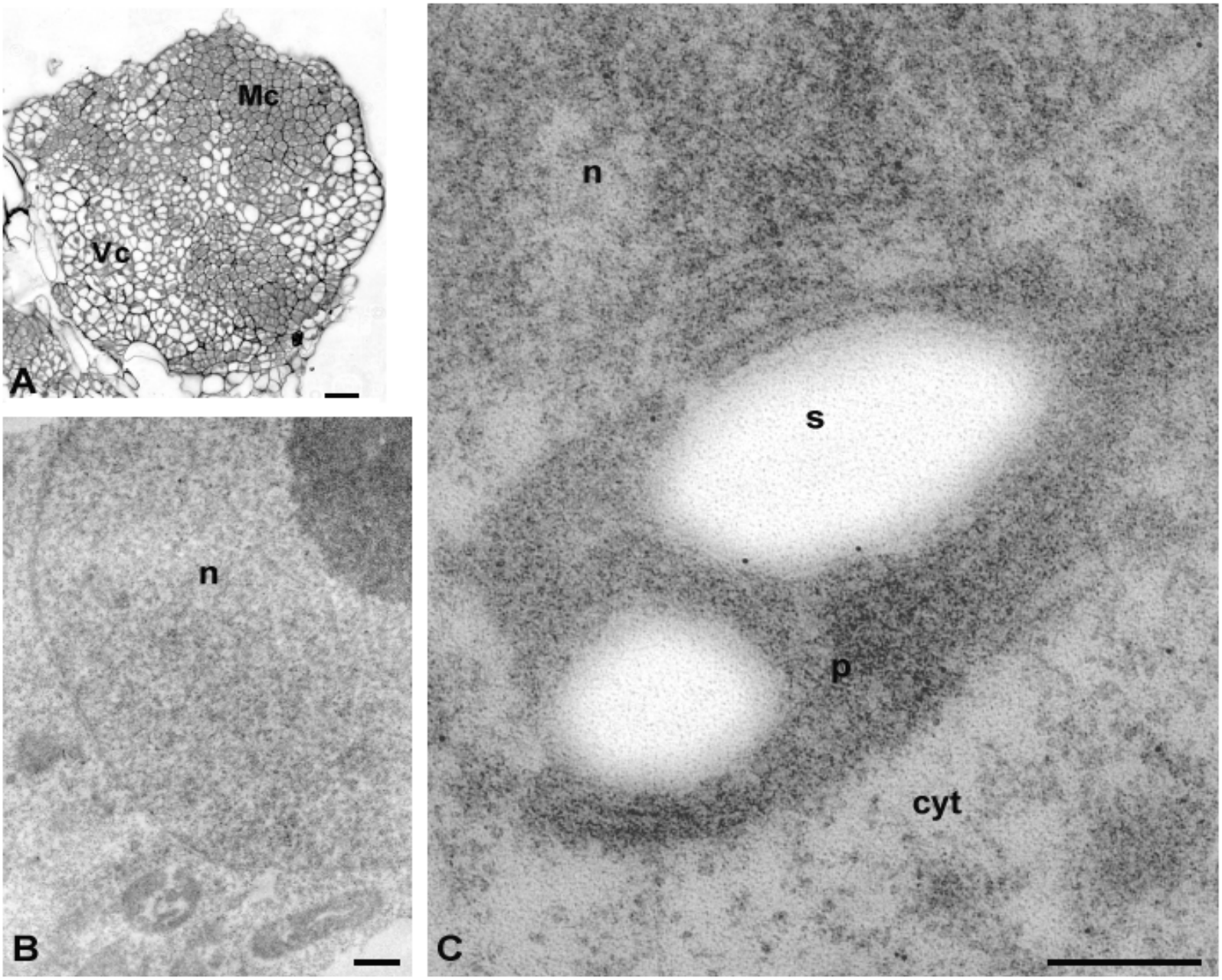

Joana Costa
Fig. 4

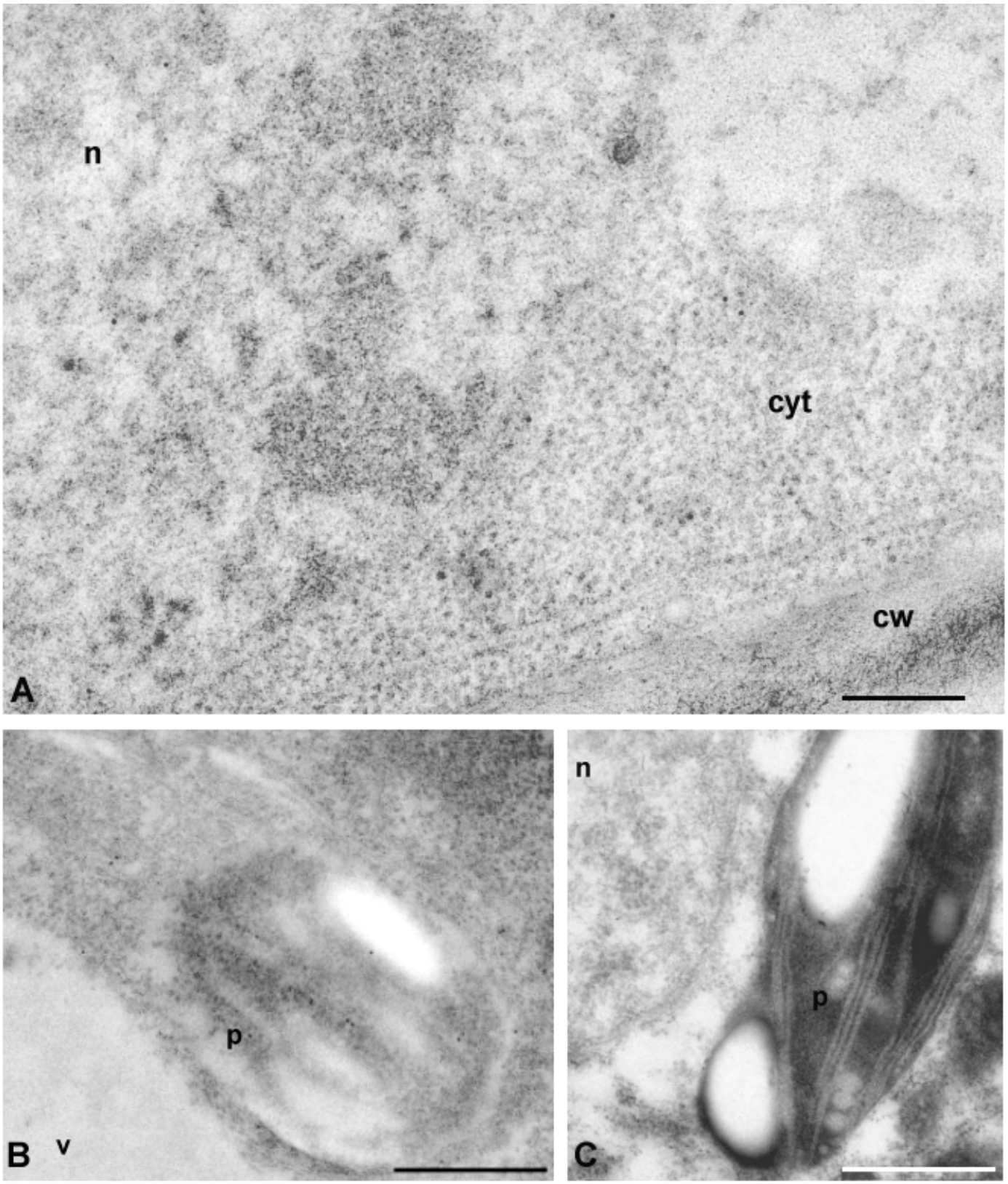
n
cyt
cw
A
p
B
v
n
p
C

Joana Costa
Fig. 5

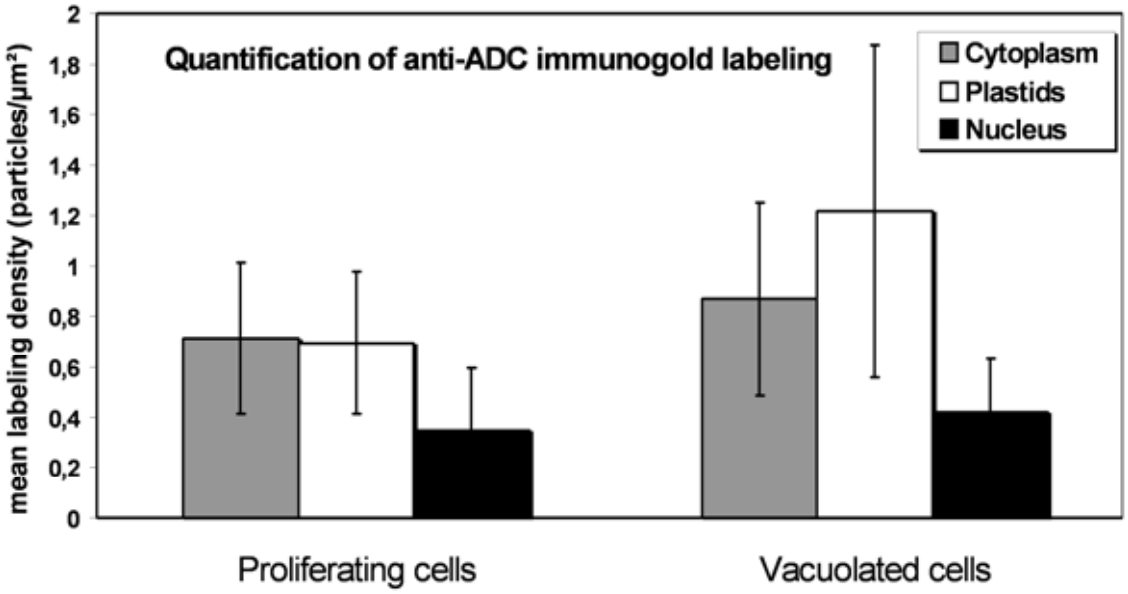

Joana Costa
Fig. 6

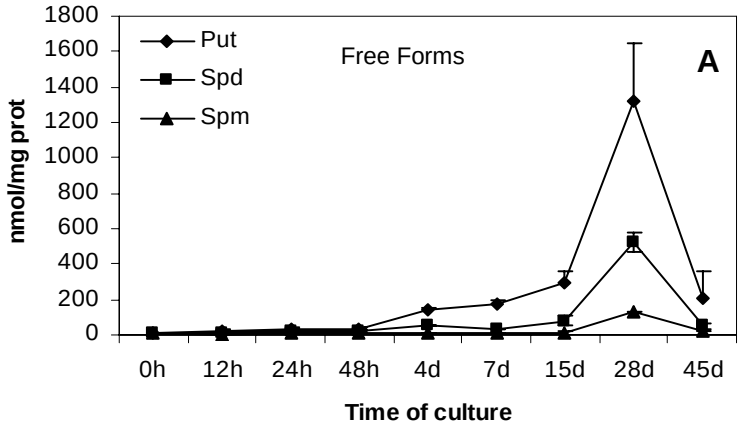

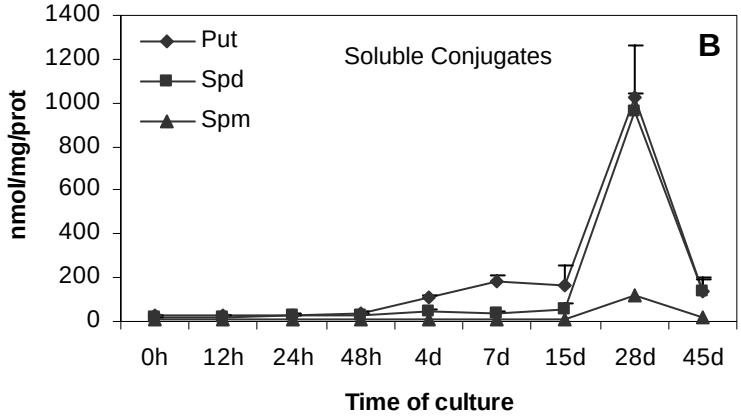

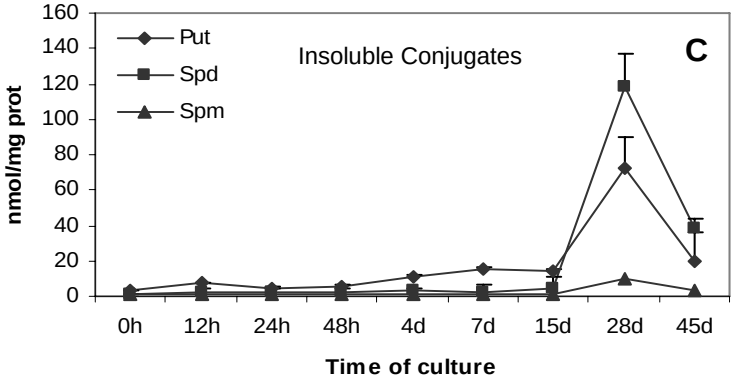

Joana Costa
Fig. 7

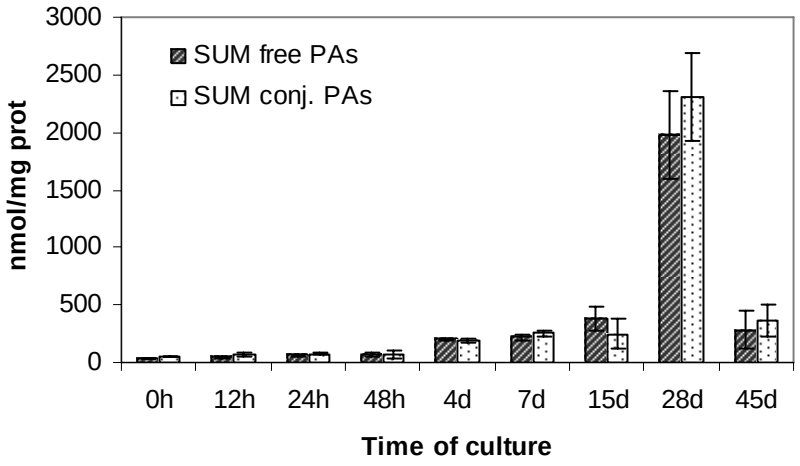

Joana Costa
Fig. 8